

Subsystem-Based Control with Modularity for Strict-Feedback Form Nonlinear Systems

Janne Koivumäki¹, Jukka-Pekka Humaloja², Lassi Paunonen², Wen-Hong Zhu³
and Jouni Mattila¹

Abstract

This study proposes an adaptive *subsystem-based control* (SBC) for systematic and straightforward nonlinear control of n th-order strict-feedback form (SFF) systems. By decomposing the SFF system to subsystems, a generic term (namely *stability connector*) can be created to address dynamic interactions between the subsystems. This 1) enables modular control design with global asymptotic stability, 2) such that both the control design and the stability analysis can be performed locally at a subsystem level, 3) while avoiding an excessive growth of the control design complexity when the system order n increases. The latter property makes the method suitable especially for high-dimensional systems. We also design a smooth projection function for addressing system parametric uncertainties. Numerical simulations demonstrate the efficiency of the method.

Index Terms

Nonlinear control, model-based control, adaptive control, globally asymptotic stability, modular control.

I. INTRODUCTION

NONLINEAR model-based control aims to design a specific feedforward (FF) compensation term based on the system inverse dynamics to generate the control output(s) from the system states and desired input signals [1]. If the FF compensation can exactly capture the inverse of the plant dynamics for all frequencies, an infinite control bandwidth with zero tracking error becomes theoretically possible [2], [3]. While early control methods, e.g., *feedback linearization* [4], aimed to cancel (or linearize) the system nonlinearities, *adaptive backstepping* [5] became a significant breakthrough in nonlinear systems control by incorporating the nonlinearities towards ideal FF compensation with *global asymptotic stability*.

This study proposes globally asymptotically stable adaptive *subsystem-based control* (SBC) for n th-order strict-feedback form (SFF) systems. The proposed method has built-in modularity and it avoids excessive growth of the control design complexity when the system order n increases (an issue reported for backstepping-based methods in several studies [6]–[9]). *Dynamic surface control* (DSC) [6], [7] and *adaptive DSC* [8] are previously developed as an alternative to backstepping to avoid the reported “explosion of complexity” with semi-global stability. They are based on *multiple sliding surface* (MSS) control [10], [11] (a method similar to backstepping) using a series of low-pass filters [7]. Our method does not employ filtering and achieves global asymptotic stability.

The proposed method originates from *virtual decomposition control* (VDC) [3], [12] that is developed for controlling complex robotic systems. *Modularity* is one of the key aspects in addressing complexity in advanced control realizations [13], [14, Sec. IV]. In VDC, robotic systems are virtually decomposed into *modular subsystems* (rigid links and joints) such that both control design and stability analysis can be performed locally at the subsystem (SS) level to guarantee overall global asymptotic stability. In particular, VDC introduced *virtual power flows* (VPFs) [3, Def. 2.16] to define dynamic interactions between the

¹J. Koivumäki and J. Mattila are with Automation and Mechanical Engineering, Faculty of Engineering and Natural Sciences, Tampere University, Finland. e-mail: firstname.surname@tuni.fi

²J.-P. Humaloja and L. Paunonen are with Mathematics, Faculty of Information Technology and Communication Sciences, Tampere University, Finland. e-mail: firstname.surname@tuni.fi

³W.-H. Zhu is with the Canadian Space Agency, Canada. e-mail: WenHong.Zhu@canada.ca

adjacent SSs such that the VPFs cancel each others out when the SSs are connected. However, when applied beyond robotics, the interactions between SSs will no longer be described by VPFs [15]. Some early ideas for the proposed method originate from the application-oriented paper in [15]. In addition, some ideological similarities can be seen to the passivity-based approach in [16] for controlling SFF systems with global asymptotic stability. While the method in [16] designed strictly passive interaction dynamics for adjacent SSs, we propose new generic tools to compensate the interaction dynamics such that every SS is automatically stabilized by its adjacent SS. More details on differences to [16] can be found in Remark 3.4.

As the main contribution, the proposed method generalizes the “subsystem-based control philosophy” in [3], [15] for controlling the n th-order SFF systems. After defining a generic form for SSs, we design a specific *stability connector* (a generic spill-over term in SS stability analysis in Def. 4.1) to address dynamic interactions between the adjacent SSs. We show that every SS with a “stability preventing” connector is compensated by the subsequent SS with a corresponding “stabilizing” connector. Similarly to VDC, we formulate a generic definition for *virtual stability*¹ such that when every SS is virtually stable, the overall system becomes automatically globally asymptotically stable. Instead of using Lebesgue L_2/L_∞ integrable functions as in [3], [15], [16], we base the results on Lyapunov functions. The proposed method is modular in the sense that control laws for every SS can be designed with a single generic-form equation as shown in Remarks 3.1 and 3.3. As part of the control design, we design a smooth projection function to address the system parametric uncertainties.

Next, Section II introduces the control problem. Section III formulates the proposed method. Section IV provides in-depth analysis on the control design and its stability. Section V provides numerical validation. Section VI concludes the study.

II. THE CONTROL PROBLEM

Consider the following n th-order SFF system

$$\begin{cases} \theta_{11}\dot{x}_1 = f_1(x_1) + g_1(x_1)x_2 & (1) \\ \theta_{i1}\dot{x}_i = f_i(\mathbf{x}_i) + g_i(\mathbf{x}_i)x_{i+1}, \forall i \in \{2, \dots, n-1\} & (2) \\ \theta_{n1}\dot{x}_n = f_n(\mathbf{x}_n) + g_n(\mathbf{x}_n)u & (3) \end{cases}$$

where $\mathbf{x}_k = [x_1, x_2, \dots, x_k]$ for all $k \in \{1, \dots, n\}$, u is the system input, $f_k(\mathbf{x}_k)$ for all $k \in \{1, \dots, n\}$ can be further written as

$$f_k(\mathbf{x}_k) = \theta_{k2}\gamma_{k2}(\mathbf{x}_k) + \theta_{k3}\gamma_{k3}(\mathbf{x}_k) + \dots + \theta_{kj}\gamma_{kj}(\mathbf{x}_k) \quad (4)$$

and $\theta_{k1}, \theta_{k2}, \dots, \theta_{kj} > 0$ in (1)–(4) are the system parameters. Similarly to backstepping, we assume that $g_k(t, \mathbf{x}_k)$ and $f_k(t, \mathbf{x}_k)$ (i.e., $\gamma_k \zeta(t, \mathbf{x}_k)$, $\forall \zeta \in \{2, \dots, j\}$) are sufficiently smooth and $g_k(t, \mathbf{x}_k) \neq 0$ on $[0, \infty) \times \mathbb{R}^k$.

Throughout the paper, we use n to denote the system overall order, while it also denotes the last SS (or its element) in (3). We use $i \in \{2, \dots, n-1\}$ to denote a SS (or its element) in the middle of the SFF sequence; see (2). We use k to denote an arbitrary decomposed SS (or its element), such that generic form for the k th SS (i.e., SS _{k}) in (1)–(3) is given by

$$\theta_{k1}\dot{x}_k = f_k(\mathbf{x}_k) + g_k(\mathbf{x}_k)x_{k+1}, \forall k \in \{1, \dots, n\} \quad (5)$$

where we denote $x_{n+1} = u$.

Let $x_{1d}(t) \in C^{n-1}(0, \infty)$ be a desired trajectory for $x_1(t)$ such that $x_{1d}^{(n)}$ exists almost everywhere. Next, our aim is to design a control for the system in (1)–(3), such that $e_1(t) = x_{1d}(t) - x_1(t)$ globally asymptotically converges to zero when $t > 0$.

¹In terms of Lyapunov functions, definition of *virtual stability* (see Def. 4.2 in Section IV) includes quadratic terms for asymptotic convergence added with stability connector(s) for compensating/stabilizing dynamics of adjacent SSs.

III. THE PROPOSED CONTROL METHOD

In Section III-A, we first design the baseline SBC by assuming the plant parameters θ_{kj} in (1)–(4) known $\forall k, \forall j$. Then, Section III-B proposes a projection function \mathcal{P}_k for parametric uncertainties, such that SBC can be updated to the proposed *adaptive* SBC in Section III-C. The control design philosophy behind the proposed method is analyzed later in Section IV.

A. Subsystem-Based Control

Assume that the system in (1)–(4) is not subject to any parametric uncertainty in θ_{kj} , $\forall k, \forall j$. The baseline SBC for the SFF system in (1)–(3) can be designed as

$$\begin{cases} g_1(x_1)x_{2d} = \theta_{11}\dot{x}_{1d} - f_1(x_1) + \lambda_1 e_1 \\ \quad = \mathbf{Y}_1 \boldsymbol{\theta}_1 + \lambda_1 e_1 & (6) \\ g_i(\mathbf{x}_i)x_{(i+1)d} = \theta_{i1}\dot{x}_{id} - f_i(\mathbf{x}_i) + \delta_{i-1}g_{i-1}(\mathbf{x}_{i-1})e_{i-1} + \lambda_i e_i \\ \quad = \mathbf{Y}_i \boldsymbol{\theta}_i + \delta_{i-1}g_{i-1}(\mathbf{x}_{i-1})e_{i-1} + \lambda_i e_i & (7) \\ g_n(\mathbf{x}_n)u = \theta_{n1}\dot{x}_{nd} - f_n(\mathbf{x}_n) + \delta_{n-1}g_{n-1}(\mathbf{x}_{n-1})e_{n-1} + \lambda_n e_n \\ \quad = \mathbf{Y}_n \boldsymbol{\theta}_n + \delta_{n-1}g_{n-1}(\mathbf{x}_{n-1})e_{n-1} + \lambda_n e_n & (8) \end{cases}$$

where $\lambda_k e_k = \lambda_k(x_{kd} - x_k)$ is the *local feedback* (FB) term with $\lambda_k > 0$; $\delta_{k-1}g_{k-1}(\mathbf{x}_{k-1})e_{k-1}$ is the *stabilizing FB* term for the previous subsystem, $\delta_{k-1} > 0$; $f_k(\mathbf{x}_k)$ is defined in (4); and in the model-based FF compensation term $\mathbf{Y}_k \boldsymbol{\theta}_k$, the regressor \mathbf{Y}_k and the parameter vector $\boldsymbol{\theta}_k$ are defined as

$$\mathbf{Y}_k := [\dot{x}_{kd}, -\gamma_{k2}(\mathbf{x}_k), -\gamma_{k3}(\mathbf{x}_k), \dots, -\gamma_{kj}(\mathbf{x}_k)] \in \mathbb{R}^{1 \times j} \quad (9)$$

$$\boldsymbol{\theta}_k := [\theta_{k1}, \theta_{k2}, \theta_{k3}, \dots, \theta_{kj}]^T \in \mathbb{R}^j. \quad (10)$$

Similarly to backstepping, $x_{(k+1)d}$ in (6) and (7) acts as a fictitious control from SS_k to the subsequent SS , $\forall k \in \{1, \dots, n-1\}$. The real control effort u can be obtained from (8) after stepping through every SS .

Remark 3.1: Similarly to SS_k dynamics in (5), the control in (6)–(8) can be reproduced with a generic and modular equation

$$g_k(\mathbf{x}_k)x_{(k+1)d} = \mathbf{Y}_k \boldsymbol{\theta}_k + \delta_{k-1}g_{k-1}(\mathbf{x}_{k-1})e_{k-1} + \lambda_k e_k$$

$\forall k \in \{1, \dots, n\}$, such that $\delta_0 g_0(\mathbf{x}_0)e_0 = 0$ and $x_{(n+1)d} = u$. The modularity in the control provides that changing SS_k dynamics, or adding/removing SS s, do not alter the structure of control laws in the remaining SS s.

B. The Proposed Smooth Projection Function

Definition 3.1: A piecewise-continuous function $\mathcal{P}_k(\mathbf{p}(t), \rho, \sigma, a, b, c, t) \in \mathbb{R}$ is a k th-order differentiable scalar function, $\forall k \in \{1, \dots, n\}$, defined for $t \geq 0$ such that its time derivative is governed by

$$\dot{\mathcal{P}}_k = \rho(\mathbf{p}(t) + \sigma \boldsymbol{\kappa}) \quad (11)$$

where $\rho, \sigma > 0$, $\mathbf{p}(t) \in C^{n-k}(0, \infty; \mathbb{R})$, $\forall k \in \{1, \dots, n\}$, and

$$\boldsymbol{\kappa} = \begin{cases} (b - \mathcal{P}_k), & \text{if } \mathcal{P}_k \geq b + c \\ (b - \mathcal{P}_k)S_b(\mathcal{P}_k), & \text{if } b < \mathcal{P}_k < b + c \\ 0, & \text{if } a \leq \mathcal{P}_k \leq b \\ (a - \mathcal{P}_k)S_a(\mathcal{P}_k), & \text{if } a - c < \mathcal{P}_k < a \\ (a - \mathcal{P}_k), & \text{if } \mathcal{P}_k \leq a - c \end{cases}$$

where $a, b, c > 0$ satisfy $c + b > b \geq a > a - c > 0$; $S_a(\mathcal{P}_k) \in C^{n-k} : (a - c, a) \rightarrow (1, 0)$ is *strictly decreasing*; and $S_b(\mathcal{P}_k) \in C^{n-k} : (b, b + c) \rightarrow (0, 1)$ is *strictly increasing*.

A solution for the switching functions $S_a(\mathcal{P}_k)$ and $S_b(\mathcal{P}_k)$ can be found in Appendix A that also provides a detailed analysis on the projection function \mathcal{P}_k and its properties.

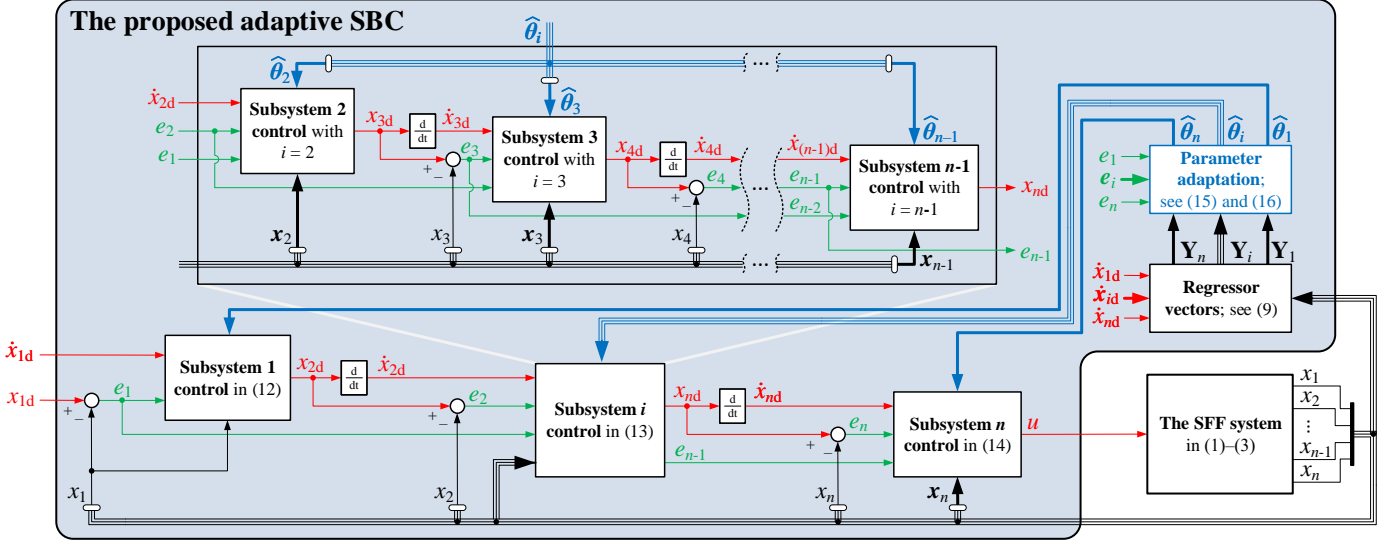


Fig. 1. Diagram of the proposed adaptive SBC (highlighted in light blue). The desired variables (and the control output u) are shown in red, the feedback signals are in green, the adaptive control is in blue, and the system output states are in black. The bold lines are vectors and the thin lines are scalar variables.

C. Adaptive Subsystem-Based Control

Let the system in (1)–(4) be subject to parametric uncertainties, i.e., θ_{kj} is unknown $\forall k, \forall j$. The control in Section III-A can be updated to the proposed *adaptive SBC* as

$$\begin{cases} g_1(x_1)x_{2d} = \mathbf{Y}_1\hat{\boldsymbol{\theta}}_1 + \lambda_1e_1 & (12) \\ g_i(\mathbf{x}_i)x_{(i+1)d} = \mathbf{Y}_i\hat{\boldsymbol{\theta}}_i + \delta_{i-1}g_{i-1}(\mathbf{x}_{i-1})e_{i-1} + \lambda_ie_i & (13) \\ g_n(\mathbf{x}_n)u = \mathbf{Y}_n\hat{\boldsymbol{\theta}}_n + \delta_{n-1}g_{n-1}(\mathbf{x}_{n-1})e_{n-1} + \lambda_ne_n & (14) \end{cases}$$

where $\mathbf{Y}_k\hat{\boldsymbol{\theta}}_k$ is the adaptive model-based FF compensation, \mathbf{Y}_k is defined in (9) and $\hat{\boldsymbol{\theta}}_k \in \mathbb{R}^j$ is an estimate of $\boldsymbol{\theta}_k$ in (10). The estimated parameters in $\hat{\boldsymbol{\theta}}_k$ need to be updated. We define

$$\mathbf{p}_k := e_k \mathbf{Y}_k^T \quad (15)$$

such that the ζ th element of $\hat{\boldsymbol{\theta}}_k$ in (12)–(14) can be updated by using the projection function \mathcal{P}_k in Definition 3.1 as

$$\hat{\theta}_{k\zeta} = \mathcal{P}_k(p_{k\zeta}, \rho_{k\zeta}, \sigma_{k\zeta}, \underline{\theta}_{k\zeta}, \bar{\theta}_{k\zeta}, c_{k\zeta}, t), \forall \zeta \in \{1, \dots, j\} \quad (16)$$

where $\hat{\theta}_{k\zeta}$ is the ζ th element of $\hat{\boldsymbol{\theta}}_k$; $p_{k\zeta}$ is the ζ th element of \mathbf{p}_k in (15); $\rho_{k\zeta} > 0$ and $\sigma_{k\zeta} > 0$ are the parameter update gains; $\underline{\theta}_{k\zeta}$ and $\bar{\theta}_{k\zeta}$ are the lower and the upper bounds of $\theta_{k\zeta}$; and $c_{k\zeta}$ defines the activation interval beyond the bounds.

Fig. 1 shows the diagram of the proposed method.

Remark 3.2: As Fig. 1 and (12)–(14) show, $\hat{\boldsymbol{\theta}}_k$ in SS_k should be continuously differentiable in C^{n-k} when stepping through the remaining SS s. The projection function \mathcal{P}_k in (11) satisfies $\hat{\boldsymbol{\theta}}_k \in C^{n-k}$, $\forall k \in \{1, \dots, n\}$. If SS_k satisfies $n-k \leq 1$, a projection function $\mathcal{P} \in C^1$ in [3], [17] can be used instead of \mathcal{P}_k . If SS_k satisfies $n-k \leq 2$, $\mathcal{P}_2 \in C^2$ in [3], [17] can be used.

Remark 3.3: As in Remark 3.1, SS_k control in (12)–(14) can be reproduced with a generic and modular equation

$$g_k(\mathbf{x}_k)x_{(k+1)d} = \mathbf{Y}_k\hat{\boldsymbol{\theta}}_k + \delta_{k-1}g_{k-1}(\mathbf{x}_{k-1})e_{k-1} + \lambda_k e_k$$

$\forall k \in \{1, \dots, n\}$, such that $\delta_0 g_0(\mathbf{x}_0)e_0 = 0$ and $x_{(n+1)d} = u$. The modularity in the control provides that changing SS_k dynamics, or adding/removing SSs, do not alter the structure of control laws in the remaining SSs.

Remark 3.4: As the main difference to [16], we design stabilizing FB term $\delta_{k-1}g_{k-1}(\mathbf{x}_{k-1})e_{k-1}$, $\forall k \in \{2, \dots, n\}$, in (12)–(14) to produce *stability connector* s_{k-1} (analyzed next in Section IV), such that passivity between SSs do not need to be considered. While the results in [16] are based on Lebesgue L_2/L_∞ integrable functions, we base the results on Lyapunov functions. We also proposed novel projection function \mathcal{P}_k in Definition 3.1 to address the system parametric uncertainties.

IV. STABILITY ANALYSIS

Next, we provide an in-depth analysis on the adaptive SBC in Section III-C. Respective analysis can be performed for the SBC in Section III-A using $\boldsymbol{\theta}_k - \boldsymbol{\theta}_k = 0$ instead of $\boldsymbol{\theta}_k - \hat{\boldsymbol{\theta}}_k$.

Motivated by a key concept in virtual stability analysis—a *virtual power flow* [3, Sect. 2.9.2]—we introduce a related notion of a *stability connector* as follows:

Definition 4.1: For the system (1)–(3) with the control (12)–(14), the *stability connector* s_k is defined as

$$s_k = \Delta_k g_k(t, \mathbf{x}_k) e_k e_{k+1}$$

where SS-related term $\Delta_k = 1$, if $k = 1$, and $\Delta_k = \frac{1}{\delta_1 \cdots \delta_{k-1}}$, if $k > 1$, and $\delta_1, \delta_2, \dots, \delta_{k-1} > 0$ are feedback gains from Section III.

Next, in Lemmas 4.1–4.3 we provide auxiliary results for the convergence analysis in Theorem 4.1. Motivated by the concept of *virtual stability* [3, Sect. 2.9], the auxiliary analysis is carried out for the individual subsystem error dynamics e_k and the corresponding parameter estimation errors $\boldsymbol{\theta}_k - \hat{\boldsymbol{\theta}}_k$.

Subtracting (1) from (12), adding $\boldsymbol{\theta}_{11}\dot{x}_{1d} - \boldsymbol{\theta}_{11}\dot{x}_{1d} = 0$, using (4), (9) and (10), and rearranging the terms, we get the following error dynamics for SS_1

$$\boldsymbol{\theta}_{11}\dot{e}_1 = -\lambda_1 e_1 + g_1(x_1)e_2 + \mathbf{Y}_1(\boldsymbol{\theta}_1 - \hat{\boldsymbol{\theta}}_1). \quad (17)$$

Lemma 4.1: Considering SS_1 error dynamics in (17), and $\boldsymbol{\theta}_1 - \hat{\boldsymbol{\theta}}_1$ governed by (10), (15) and (16), the derivative of the quadratic function

$$v_1 = \frac{1}{2} \left(\boldsymbol{\theta}_{11} e_1^2 + \sum_{\zeta=1}^j \frac{(\boldsymbol{\theta}_{1\zeta} - \hat{\boldsymbol{\theta}}_{1\zeta})^2}{\rho_{1\zeta}} \right) \quad (18)$$

along the trajectories of the error dynamics satisfies

$$\dot{v}_1 \leq -\lambda_1 e_1^2 + s_1 \quad (19)$$

where s_1 is the stability connector from Definition 4.1.

Proof: See Appendix B. ■

Remark 4.1: In Lemma 4.1, term e_2 in (17) is treated as an external input that causes s_1 to appear in (19) (see Appendix B) that will be canceled out based on the result of the next lemma. The dynamics of e_2 as well as the subsequent subsystems error dynamics are accounted for in the next two lemmas.

Subtracting (2) from (13), adding $\boldsymbol{\theta}_{i1}\dot{x}_{id} - \boldsymbol{\theta}_{i1}\dot{x}_{id} = 0$ using (4), (9) and (10), and rearranging the terms, we get the following error dynamics for SS_i , $\forall i \in \{2, \dots, n-1\}$,

$$\begin{aligned} \boldsymbol{\theta}_{i1}\dot{e}_i &= -\lambda_i e_i - \delta_{i-1}g_{i-1}(\mathbf{x}_{i-1})e_{i-1} + g_i(\mathbf{x}_i)e_{i+1} \\ &\quad + \mathbf{Y}_i(\boldsymbol{\theta}_i - \hat{\boldsymbol{\theta}}_i). \end{aligned} \quad (20)$$

Lemma 4.2: Considering SS_i error dynamics in (20), and $\boldsymbol{\theta}_i - \hat{\boldsymbol{\theta}}_i$ governed by (10), (15) and (16), the derivative of the quadratic function

$$v_i = \frac{1}{2(\delta_1 \cdots \delta_{i-1})} \left(\boldsymbol{\theta}_{i1} e_i^2 + \sum_{\zeta=1}^j \frac{(\boldsymbol{\theta}_{i\zeta} - \hat{\boldsymbol{\theta}}_{i\zeta})^2}{\rho_{i\zeta}} \right) \quad (21)$$

along the trajectories of the error dynamics satisfies

$$\dot{v}_i \leq -\frac{\lambda_i}{\delta_1 \cdots \delta_{i-1}} e_i^2 - s_{i-1} + s_i \quad (22)$$

where s_{i-1} and s_i are the stability connectors from Definition 4.1.

Proof: See Appendix B. ■

Remark 4.2: Similarly to Lemma 4.1, e_{i+1} in (20) is treated as an external input that causes s_i to appear in (22). The stabilizing FB term $\delta_{i-1}g_{i-1}(\mathbf{x}_{i-1})e_{i-1}$ in (20) creates another stability connector $-s_{i-1}$ to appear in (22) (see Appendix B) that will cancel out s_{i-1} from the previous SS. The last connector s_{n-1} will be canceled out based on the result of the next lemma, after which we are in the position to present the convergence result for the overall error dynamics.

Subtracting (3) from (14), adding $\theta_{n1}\dot{x}_{nd} - \theta_{n1}\dot{x}_{nd} = 0$ using (4), (9) and (10), and rearranging the terms, we get the following error dynamics for SS_n

$$\theta_{n1}\dot{e}_n = -\lambda_n e_n - \delta_{n-1}g_{n-1}(\mathbf{x}_{n-1})e_{n-1} + \mathbf{Y}_n(\boldsymbol{\theta}_n - \widehat{\boldsymbol{\theta}}_n). \quad (23)$$

Lemma 4.3: Considering SS_n error dynamics in (23), and $\boldsymbol{\theta}_n - \widehat{\boldsymbol{\theta}}_n$ governed by (10), (15) and (16), the derivative of the quadratic function

$$v_n = \frac{1}{2(\delta_1 \cdots \delta_{n-1})} \left(\theta_{n1} e_n^2 + \sum_{\zeta=1}^j \frac{(\theta_{n\zeta} - \widehat{\theta}_{n\zeta})^2}{\rho_{n\zeta}} \right) \quad (24)$$

along the trajectories of the error dynamics satisfies

$$\dot{v}_n \leq -\frac{\lambda_n}{\delta_1 \cdots \delta_{n-1}} e_n^2 - s_{n-1} \quad (25)$$

where s_{n-1} is the stability connector from Definition 4.1.

Proof: See Appendix B. ■

We will now construct a Lyapunov candidate for the overall error dynamics as the sum of the quadratic functions from Lemmas 4.1–4.3. Based on the properties derived in the lemmas, we obtain that the error dynamics will remain bounded, and moreover, that the control errors converge globally asymptotically to zero. The result is given in the following theorem.

Theorem 4.1: Consider the error dynamics $\mathbf{e} = [e_1, \dots, e_n]^T$ and the parameter estimation error $\boldsymbol{\theta}_k - \widehat{\boldsymbol{\theta}}_k$, $\forall k \in \{1, 2, \dots, n\}$, that are governed in Lemmas 4.1–4.3. For arbitrary initial conditions, $\boldsymbol{\theta}_k - \widehat{\boldsymbol{\theta}}_k$ remains bounded and $e_k(t) \rightarrow 0$ globally as $t \rightarrow \infty$ for all $k \in \{1, 2, \dots, n\}$.

Proof: Using (18), (21) and (24), we choose a Lyapunov candidate function for the overall error dynamics as

$$\begin{aligned} v_{\text{tot}} &= v_1 + \sum_{i=2}^{n-1} v_i + v_n \\ &= \frac{1}{2} \mathbf{e}^T \mathbf{A} \mathbf{e} + \sum_{k=1}^n \frac{1}{2(\delta_1 \cdots \delta_{k-1})} \sum_{\zeta=1}^j \frac{(\theta_{k\zeta} - \widehat{\theta}_{k\zeta})^2}{\rho_{k\zeta}} \end{aligned}$$

where $\mathbf{A} = \text{diag} \left(\theta_{11}, \frac{\theta_{21}}{\delta_1}, \frac{\theta_{31}}{\delta_1 \delta_2}, \dots, \frac{\theta_{n1}}{\delta_1 \cdots \delta_{n-1}} \right) \in \mathbb{R}^{n \times n}$ is positive definite. Then, it follows from (19), (22) and (25) that

$$\begin{aligned} \dot{v}_{\text{tot}} &= \dot{v}_1 + \sum_{i=2}^{n-1} \dot{v}_i + \dot{v}_n \\ &\leq -\lambda_1 e_1^2 + s_1 - \sum_{i=2}^{n-1} \left[\frac{\lambda_i}{\delta_1 \cdots \delta_{i-1}} e_i^2 - s_{i-1} + s_i \right] - \frac{\lambda_n}{\delta_1 \cdots \delta_{n-1}} e_n^2 - s_{n-1} \end{aligned}$$

$$\begin{aligned}
&= -\lambda_1 e_1^2 - \sum_{i=2}^{n-1} \frac{\lambda_1}{\delta_1 \cdots \delta_{i-1}} e_i^2 - \frac{\lambda_n}{\delta_1 \cdots \delta_{n-1}} e_n^2 + \sum_{k=1}^{n-1} (s_k - s_k) \\
&= -\mathbf{e}^T \mathbf{B} \mathbf{e}
\end{aligned}$$

where $\mathbf{B} = \text{diag} \left(\lambda_1, \frac{\lambda_2}{\delta_1}, \frac{\lambda_3}{\delta_1 \delta_2}, \dots, \frac{\lambda_n}{\delta_1 \cdots \delta_{n-1}} \right) \in \mathbb{R}^{n \times n}$ is positive definite and every stability connector s_k is canceled by its negative counterpart $-s_k, \forall k \in \{1, 2, \dots, n-1\}$. By [18, Thm. 8.4] both the control errors and the parameter estimation errors are bounded, and $\mathbf{e}(t)^T \mathbf{B} \mathbf{e}(t) \rightarrow 0$ globally as $t \rightarrow \infty$, which by the positive-definiteness of \mathbf{B} is equivalent to $\mathbf{e}(t) \rightarrow \mathbf{0}$ as $t \rightarrow \infty$, i.e., $e_k(t) \rightarrow 0, \forall k \in \{1, 2, \dots, n\}$ as $t \rightarrow \infty$. ■

Finally, motivated by the original concept of *virtual stability* [3, Sect. 2.9], Definition 4.2 generalizes the results in Lemmas 4.1–4.3 for *virtual stability* of the k th subsystem.

Definition 4.2: The k th subsystem, $\forall k \in \{1, \dots, n\}$, in (1)–(3), combined with its respective control in (12)–(16), is said to be *virtually stable* if the derivative of a quadratic function $v_k = \alpha_k e_k^2 + (\boldsymbol{\theta}_k - \widehat{\boldsymbol{\theta}}_k)^T \boldsymbol{\Gamma}_k (\boldsymbol{\theta}_k - \widehat{\boldsymbol{\theta}}_k)$ along the trajectories of the error dynamics satisfies $\dot{v}_k \leq -\beta_k e_k^2 - s_{k-1} + s_k$ for some $\alpha_k, \beta_k > 0$ and positive-definite $\boldsymbol{\Gamma}_k \in \mathbb{R}^{k \times k}$, where s_{k-1} and s_k are the stability connectors by Def. 4.1 such that $s_0 = 0$ and $s_n = 0$.

Remark 4.3: Definition 4.2 provides generic tools to design local subsystem-based control for SFF systems. As we demonstrated in Theorem 4.1, *virtual stability* of every SS in the sense of Definition 4.2 (derived from Lemmas 4.1–4.3) guarantees *global asymptotic stability* of the overall system.

V. NUMERICAL VALIDATION

In order to validate the proposed method, we consider the 3rd order nonlinear system from [8], [9], namely,

$$\begin{cases} \dot{x}_1 = a_1 x_1^3 + x_2 \\ \dot{x}_2 = a_2 (x_1^2 + x_2^2) + x_3 \\ \dot{x}_3 = u. \end{cases} \quad (26)$$

Using (12)–(14), the proposed adaptive SBC for the system in (26) can be designed as

$$\begin{cases} x_{2d} = \mathbf{Y}_1 \widehat{\boldsymbol{\theta}}_1 + \lambda_1 e_1 \\ x_{3d} = \mathbf{Y}_2 \widehat{\boldsymbol{\theta}}_2 + \lambda_2 e_2 + \delta_1 e_1 \\ u = \mathbf{Y}_3 \widehat{\boldsymbol{\theta}}_3 + \lambda_3 e_3 + \delta_2 e_2 \end{cases} \quad (27)$$

where $\mathbf{Y}_1 = [\dot{x}_{1d} \quad -x_1^3]$, $\boldsymbol{\theta}_1 = [1 \quad \theta_{12}]^T$, $\mathbf{Y}_2 = [\dot{x}_{2d} \quad -(x_1^2 + x_2^2)]$, $\boldsymbol{\theta}_2 = [1 \quad \theta_{22}]^T$, $\mathbf{Y}_3 = \dot{x}_{3d}$ and $\boldsymbol{\theta}_3 = \theta_{31} = 1$. The parameters in $\widehat{\boldsymbol{\theta}}_k, \forall k \in \{1, 2, 3\}$, are updated with \mathcal{P}_k in Definition 3.1. For simplicity, only parameters θ_{12} and θ_{22} (corresponding a_1 and a_2 in the plant) are adapted in the experiments, although possibility to adapt $\theta_{k1} = 1, \forall k \in \{1, 2, 3\}$, remains.

To study the global asymptotic convergence suggested by Theorem 4.1, the following piecewise differentiable and sufficiently smooth reference trajectory $x_{1d}(t)$ is used

$$x_{1d}(t) = \begin{cases} \sin(2\pi t) \tanh(t^3), & \text{if } 0 \leq t \leq 5 \\ \sin(2\pi t) \tanh(t^3) [1 - \tanh((t-5)^3)], & \text{if } t > 5. \end{cases}$$

Throughout the simulations, $a_1 = 5$ and $a_2 = 5$ are used for the plant in (26), and the FB gains were loosely tuned to $\lambda_1 = 10$, $\lambda_2 = 20$, $\lambda_3 = 40$, $\delta_1 = 10$ and $\delta_2 = 20$. The sample time in simulations was set to 0.01 ms to address the exponential rate of dynamics. The following three test cases are studied:

C1: The baseline SBC (in Sec. III-A) is employed, i.e., $\boldsymbol{\theta}_1$, $\boldsymbol{\theta}_2$ and $\boldsymbol{\theta}_3$ (instead of $\widehat{\boldsymbol{\theta}}_1$, $\widehat{\boldsymbol{\theta}}_2$ and $\widehat{\boldsymbol{\theta}}_3$) are used in (27). In addition, inaccurate FF parameters $\theta_{12} = 6$ and $\theta_{22} = 4$ are used in relation to their respective plant parameters $a_1 = 5$ and $a_2 = 5$ in (26). Figs. 2 and 3 show the results.

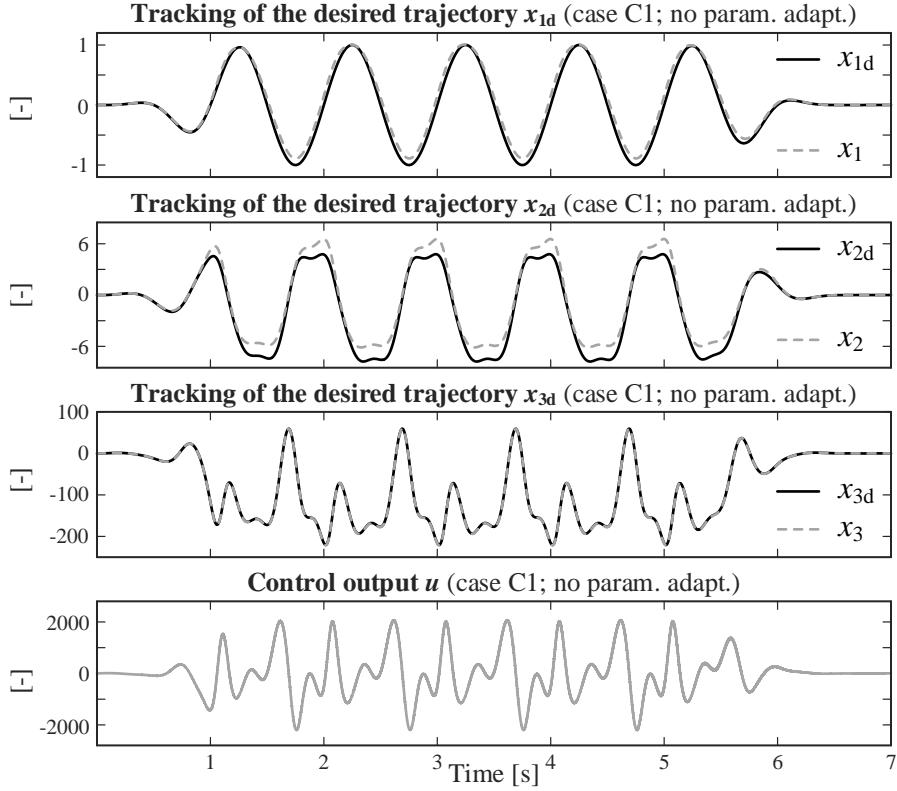


Fig. 2. Control performance in C1 with inaccurate parameter values $\theta_{12} = 6$ and $\theta_{22} = 4$ in relation to the actual plant parameters $a_1 = 5$ and $a_2 = 5$. The desired trajectories are shown in black and their controlled variables in gray (plots 1–3). The last plot shows the control output u .

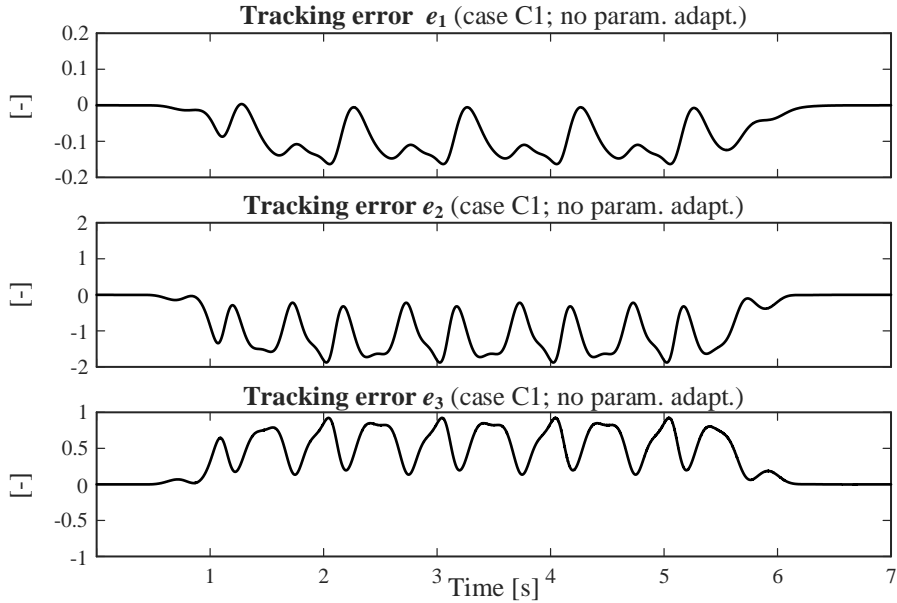


Fig. 3. Tracking errors e_k , $\forall k \in \{1, 2, 3\}$, in C1 (adaptive control disabled).

C2: The proposed adaptive SBC (in Sec. III-C) is employed with initial parameter estimate values $\hat{\theta}_{12}(0) = 6$ and $\hat{\theta}_{22}(0) = 4$ in (27). Figs. 4–6 show the results.

C3: The proposed adaptive SBC (in Sec. III-C) is employed with initial parameter estimate values $\hat{\theta}_{12}(0) = 0.1$ and $\hat{\theta}_{22}(0) = 9.9$. Figs. 5 and 6 show the results.

In cases C2 and C3 with the adaptive control, the parameter update gains were set to $\rho_{12} = 1000$, $\sigma_{12} =$

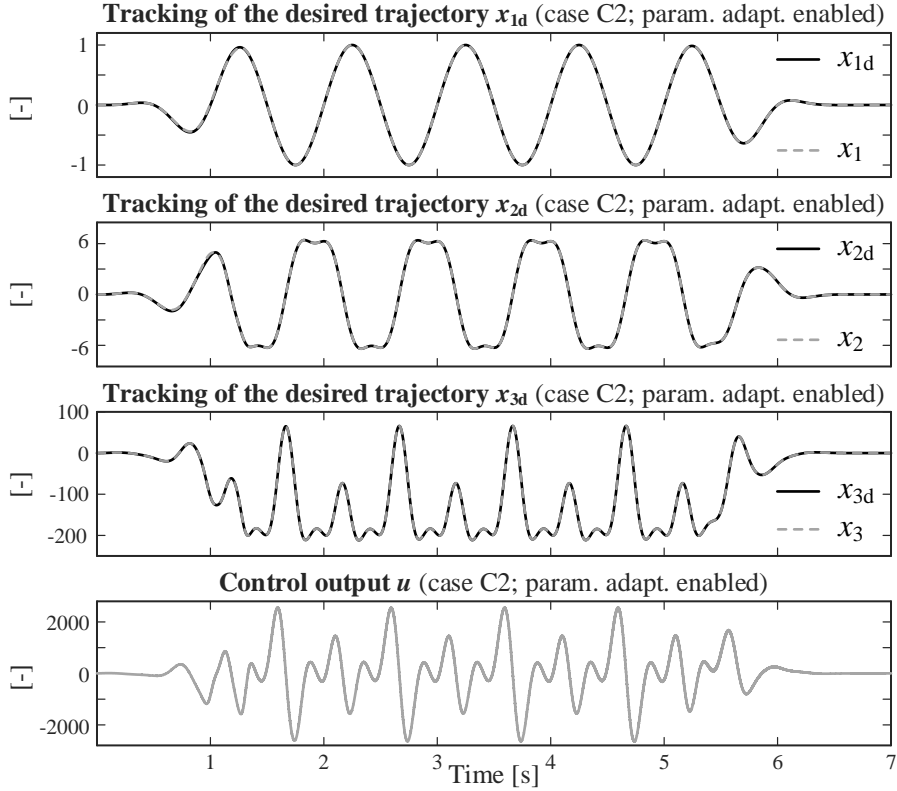


Fig. 4. Control performance in C2 with initial parameter values $\hat{\theta}_{12}(0) = 6$ and $\hat{\theta}_{22}(0) = 4$, while $a_1 = 5$ and $a_2 = 5$ hold for the respective plant parameters. The desired trajectories are shown in black and their controlled variables in gray (plots 1–3). The last plot shows the control output u .

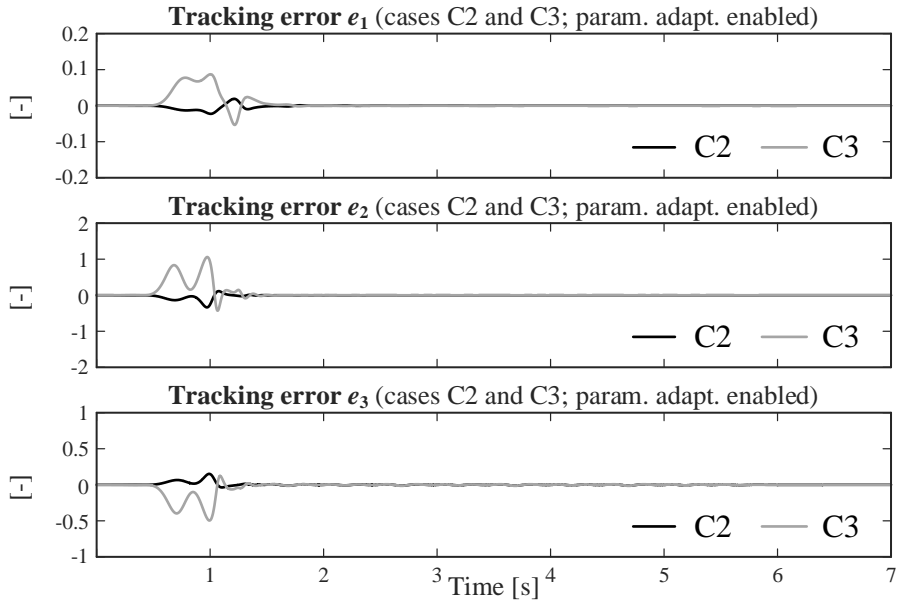


Fig. 5. Tracking errors e_k , $\forall k \in \{1, 2, 3\}$, in C2 and C3 (adaptive control enabled). The results in C2 are in black and the results in C3 are in gray.

$1000/\rho_{12}$, $\rho_{22} = 2$ and $\sigma_{22} = 1000/\rho_{22}$; the parameter bounds were set to $\bar{\theta}_{12} = 9$, $\underline{\theta}_{12} = 1$, $\bar{\theta}_{22} = 9$ and $\underline{\theta}_{22} = 1$; and the activation intervals beyond the bounds were set to 0.5 ($c_{21} = 0.5$ and $c_{22} = 0.5$)

Figs. 2 and 3 show the results in case C1, where the control for the plant is designed by the theory in Section III-A. However, inaccurate FF parameters (i.e., $\theta_{12} \neq a_1$ and $\theta_{22} \neq a_2$) are used such that, in cases C2 and C3, comparisons can be made to the proposed adaptive SBC. In plots 1–3, Fig. 2 shows the

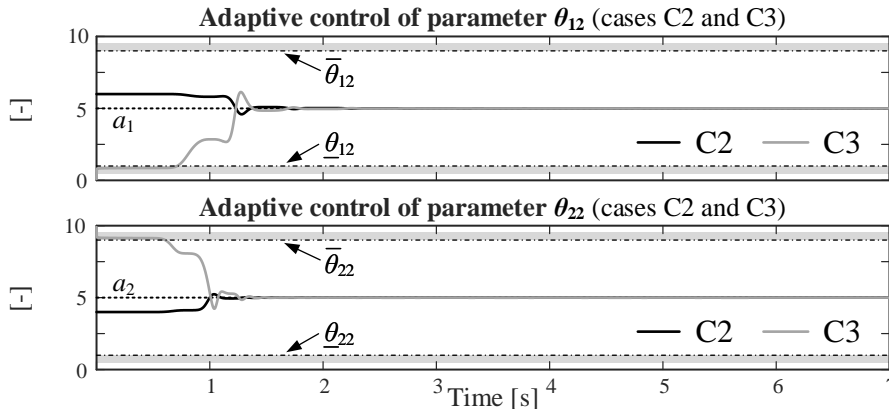


Fig. 6. Adapted parameters $\hat{\theta}_{12}(t)$ (the 1st plot) and $\hat{\theta}_{22}(t)$ (the 2nd plot). The results in C2 ($\hat{\theta}_{12}(0) = 6$ and $\hat{\theta}_{22}(0) = 4$) are given in black, while the result in C3 ($\hat{\theta}_{12}(0) = 0.1$ and $\hat{\theta}_{22}(0) = 9.9$) are given in dark gray. The plant parameters $a_1 = 5$ and $a_2 = 5$ are shown in dashed line. The upper bound $\bar{\theta} = 9$ and lower bound $\underline{\theta} = 1$ are shown in dashed-dot line. The bound activation intervals (defined by $c_{21} = 0.5$ and $c_{22} = 0.5$) are in gray.

desired trajectory x_{kd} , $\forall k \in \{1, 2, 3\}$, in black and its controlled state x_k in gray. The last plot shows the control output u . The detailed tracking errors are shown in Fig. 3, the maximum absolute tracking errors being $|e_1|_{\max} = 0.163$, $|e_2|_{\max} = 1.877$ and $|e_3|_{\max} = 0.924$. As can be seen, noticeable tracking errors occur in the transition phases due to the parametric uncertainty.

Figs. 4–6 show the main results of the study with the proposed adaptive SBC in (27). Fig. 4 shows the tracking results in case C2 where the initial values for the parameter estimates are selected in accordance to case C1, i.e., $\hat{\theta}_{12}(0) = 6$ and $\hat{\theta}_{22}(0) = 4$. As the black lines in Fig. 5 shows, the tracking errors are substantially decreased in relation to case C1, with the maximum absolute tracking errors $|e_1|_{\max} = 0.023$, $|e_2|_{\max} = 0.336$ and $|e_3|_{\max} = 0.152$. As predicted by the theory, global asymptotic convergence is achieved. Fig. 6 shows the behavior of the parameter estimates $\hat{\theta}_{12}$ and $\hat{\theta}_{22}$ in black, illustrating that the proposed projection function \mathcal{P}_k actively pushes the parameter values toward their real values in the plant.

In the last case C3, the initial parameter values are set outside the projection function \mathcal{P}_k bounds such that $\hat{\theta}_{12}(0) = 0.1$ and $\hat{\theta}_{22}(0) = 9.9$. The results are shown in Figs. 5 and 6 in gray. Despite a significant inaccuracy in the initial parameter values, the projection function \mathcal{P}_k actively pushes the parameter values toward their real values in the plant (see Fig. 6), with the maximum absolute tracking errors $|e_1|_{\max} = 0.087$, $|e_2|_{\max} = 1.060$ and $|e_3|_{\max} = 0.496$ (see Fig. 5). After 1.5 s the control behavior in case C3 becomes virtually identical to case C2.

VI. CONCLUSIONS

This study proposed an *adaptive subsystem-based control* for controlling n th-order SFF systems with parametric uncertainties. As an alternative for backstepping, we provided systematic and straightforward tools for globally asymptotically stable control while avoiding a growth of the control design complexity when the system order n increases. The proposed method is modular in the sense that the control for every SS can be designed with a single generic-form equation such that changing SS dynamics or removing/adding SSs do not affect to the control laws in the remaining SSs. For the method, we reformulated the original concept of *virtual stability* in [3, Def. 2.17] and proposed a specific *stability connector* to address dynamic interactions between the adjacent SSs. These features enable that both the control design and the stability analysis can be performed locally at a SS level (as opposed to the whole system); see Remark 4.3. We proposed also a smooth projection function \mathcal{P}_k for the system parametric uncertainties. Theoretical developments on global asymptotic convergence (in Theorem 4.1) were verified in numerical simulations. Semi-SFF systems with unknown dynamics remain a subject for future studies.

APPENDIX A
THE PROJECTION FUNCTION \mathcal{P}_k

Consider the piecewise-continuous projection function \mathcal{P}_k in Definition 3.1. Parameters a and b define the lower and upper bounds for \mathcal{P}_k such that $b \geq a > 0$. Within the bounds, $\dot{\mathcal{P}}_k$ is driven by $\rho p(t)$ and the behavior of \mathcal{P}_k is equal to $\mathcal{P} \in C^1$ and $\mathcal{P}_2 \in C^2$ in [3], [17]. Outside the bounds, a corrective term $\sigma \kappa$ is designed to bring \mathcal{P}_k back toward the bounds. The parameter c defines activation interval lengths $(a-c, a)$ and $(b, b+c)$ for the switching functions $S_a(\mathcal{P}_k)$ and $S_b(\mathcal{P}_k)$.

Let $|p^{(n-k)}(t)| < +\infty, \forall k \in \{1, \dots, n\}$. To guarantee the existence of $\mathcal{P}_k^{(k)}$ outside the bounds, the switching functions $S_a(\mathcal{P}_k) : (a-c, a) \rightarrow (1, 0)$ and $S_b(\mathcal{P}_k) : (b, b+c) \rightarrow (0, 1)$ are required to satisfy the boundary conditions [in (28) and (29)]

$$\begin{aligned} \lim_{x \rightarrow (a-c)^+} S_a(x) = 1, \quad \lim_{x \rightarrow (a-c)^+} S_a^{(j)}(x) = 0, \\ \lim_{x \rightarrow a^-} S_a(x) = 0 \quad \text{and} \quad \lim_{x \rightarrow a^-} S_a^{(j)}(x) = 0, \end{aligned} \quad (28)$$

$$\begin{aligned} \lim_{x \rightarrow (b+c)^-} S_b(x) = 1, \quad \lim_{x \rightarrow (b+c)^-} S_b^{(j)}(x) = 0, \\ \lim_{x \rightarrow b^+} S_b(x) = 0 \quad \text{and} \quad \lim_{x \rightarrow b^+} S_b^{(j)}(x) = 0, \end{aligned} \quad (29)$$

$\forall j \in \{1, \dots, n-1\}$. Definition A.1 provides smooth and strictly decreasing solution for $S_a(\mathcal{P}_k)$, satisfying (28), and smooth and strictly increasing solution for $S_b(\mathcal{P}_k)$, satisfying (29).

Definition A.1: $S_a(\mathcal{P}_k) : (a-c, a) \rightarrow (1, 0)$ is a *smooth and strictly decreasing* switching function defined as

$$S_a(\mathcal{P}_k) := \frac{1}{2} \left[1 - \tanh \left(\frac{1}{a-c-\mathcal{P}_k} + \frac{1}{a-\mathcal{P}_k} \right) \right]$$

and $S_b(\mathcal{P}_k) : (b, b+c) \rightarrow (0, 1)$ is a *smooth and strictly increasing* switching function defined as

$$S_b(\mathcal{P}_k) := \frac{1}{2} \left[1 + \tanh \left(\frac{1}{b-\mathcal{P}_k} + \frac{1}{b+c-\mathcal{P}_k} \right) \right].$$

The projection function in (11) has the following property.

Lemma A.1: For any constant \mathcal{P}_c with $a \leq \mathcal{P}_c \leq b$ we have

$$(\mathcal{P}_c - \mathcal{P}_k) \left(p(t) - \frac{1}{\rho} \dot{\mathcal{P}}_k \right) \leq -\sigma \kappa^2 \leq 0. \quad (30)$$

Proof: The proof of Lemma A.1 follows a similar procedure as the proof of Lemma 2.10 in [3]. Let $a \leq \mathcal{P}_c \leq b$. Then, for a constant \mathcal{P}_c we have

$$(\mathcal{P}_c - \mathcal{P}_k) \geq (a - \mathcal{P}_k) \quad (31)$$

$$(\mathcal{P}_k - \mathcal{P}_c) \geq (\mathcal{P}_k - b). \quad (32)$$

Substituting (11) into (30) we get

$$(\mathcal{P}_c - \mathcal{P}_k) \left(p(t) - \frac{1}{\rho} \dot{\mathcal{P}}_k \right) = -\sigma (\mathcal{P}_c - \mathcal{P}_k) \kappa. \quad (33)$$

When $\mathcal{P}_n \leq a-c$, Definition 3.1 yields $\kappa = (a - \mathcal{P}_k)$. Using (31), we get

$$-\sigma (\mathcal{P}_c - \mathcal{P}_k) \kappa \leq -\sigma (a - \mathcal{P}_k) \kappa = -\sigma \kappa^2 \leq 0. \quad (34)$$

When $a - c < \mathcal{P}_k < a$, Definition 3.1 yields $\kappa = (a - \mathcal{P}_k)S_a(\mathcal{P}_k)$ and $S_a(\mathcal{P}_k) \in (0, 1)$. Using (31), we get

$$\begin{aligned} -\sigma(\mathcal{P}_c - \mathcal{P}_k)\kappa &\leq -\sigma(a - \mathcal{P}_k)\kappa \\ &< -\sigma(a - \mathcal{P}_k)S_a(\mathcal{P}_k)\kappa \\ &= -\sigma\kappa^2 \leq 0. \end{aligned} \quad (35)$$

When $a \leq \mathcal{P}_k \leq b$, Definition 3.1 yields $\kappa = 0$ and we get

$$-\sigma(\mathcal{P}_c - \mathcal{P}_k)\kappa = 0. \quad (36)$$

When $b < \mathcal{P}_k < b + c$, Definition 3.1 yields $\kappa = (b - \mathcal{P}_k)S_b(\mathcal{P}_k)$ and $S_b(\mathcal{P}_k) \in (0, 1)$. Using (32), we get

$$\begin{aligned} -\sigma(\mathcal{P}_c - \mathcal{P}_k)\kappa &= \sigma(\mathcal{P}_k - \mathcal{P}_c)\kappa \\ &\leq \sigma(\mathcal{P}_k - b)\kappa \\ &< \sigma(\mathcal{P}_k - b)S_b(\mathcal{P}_k)\kappa \\ &= -\sigma(b - \mathcal{P}_k)S_b(\mathcal{P}_k)\kappa \\ &= -\sigma\kappa^2 \leq 0. \end{aligned} \quad (37)$$

When $\mathcal{P}_k \geq b + c$, Definition 3.1 yields $\kappa = (b - \mathcal{P}_k)$. Using (32), we get

$$\begin{aligned} -\sigma(\mathcal{P}_c - \mathcal{P}_k)\kappa &= \sigma(\mathcal{P}_k - \mathcal{P}_c)\kappa \\ &\leq \sigma(\mathcal{P}_k - b)\kappa \\ &= -\sigma(b - \mathcal{P}_k)\kappa \\ &= -\sigma\kappa^2 \leq 0. \end{aligned} \quad (38)$$

Finally, (34)–(38) together with (33) complete the proof. \blacksquare

APPENDIX B

PROOFS OF LEMMAS 4.1, 4.2, AND 4.3

Proof of Lemma 4.1: Using (17), Definition 4.1 and Lemma A.1, the derivative of the quadratic function v_1 in (18) can be written as

$$\begin{aligned} \dot{v}_1 &= e_1 \theta_{11} \dot{e}_1 - \sum_{\zeta=1}^j (\theta_{1\zeta} - \hat{\theta}_{1\zeta}) \frac{\hat{\theta}_{1\zeta}}{\rho_{1\zeta}} \\ &= -\lambda_1 e_1^2 + g_1(x_1) e_1 e_2 + e_1 \mathbf{Y}_1(\boldsymbol{\theta}_1 - \hat{\boldsymbol{\theta}}_1) - \sum_{\zeta=1}^j (\theta_{1\zeta} - \hat{\theta}_{1\zeta}) \frac{\hat{\theta}_{1\zeta}}{\rho_{1\zeta}} \\ &= -\lambda_1 e_1^2 + g_1(x_1) e_1 e_2 + \sum_{\zeta=1}^j (\theta_{1\zeta} - \hat{\theta}_{1\zeta}) \left(p_{1\zeta} - \frac{\hat{\theta}_{1\zeta}}{\rho_{1\zeta}} \right) \\ &\leq -\lambda_1 e_1^2 + s_1 \end{aligned}$$

which completes the proof of Lemma 4.1. \blacksquare

Proof of Lemma 4.2: Using (20), Definition 4.1 and Lemma A.1, the derivative of the quadratic function v_i in (21), $\forall i \in \{2, \dots, n-1\}$, can be written as

$$\dot{v}_i = e_i \frac{\theta_{i1}}{\delta_1 \cdots \delta_{i-1}} \dot{e}_i - \frac{1}{\delta_1 \cdots \delta_{i-1}} \sum_{\zeta=1}^j (\theta_{i\zeta} - \hat{\theta}_{i\zeta}) \frac{\hat{\theta}_{i\zeta}}{\rho_{i\zeta}}$$

$$\begin{aligned}
&= e_i \frac{1}{\delta_1 \cdots \delta_{i-1}} \left[g_i(\mathbf{x}_i) e_{i+1} - \delta_{i-1} g_{i-1}(\mathbf{x}_{i-1}) e_{i-1} - \lambda_i e_i + \mathbf{Y}_i(\boldsymbol{\theta}_i - \widehat{\boldsymbol{\theta}}_i) \right] \\
&\quad - \frac{1}{\delta_1 \cdots \delta_{i-1}} \sum_{\zeta=1}^j (\theta_{i\zeta} - \widehat{\theta}_{i\zeta}) \frac{\widehat{\theta}_{i\zeta}}{\rho_{i\zeta}} \\
&= -\frac{\lambda_i}{\delta_1 \cdots \delta_{i-1}} e_i^2 - \frac{1}{\delta_1 \cdots \delta_{i-2}} g_{i-1}(\mathbf{x}_{i-1}) e_{i-1} e_i + \frac{1}{\delta_1 \cdots \delta_{i-1}} g_i(\mathbf{x}_i) e_i e_{i+1} \\
&\quad + \frac{1}{\delta_1 \cdots \delta_{i-1}} \sum_{\zeta=1}^j (\theta_{i\zeta} - \widehat{\theta}_{i\zeta}) \left(p_{i\zeta} - \frac{\widehat{\theta}_{i\zeta}}{\rho_{i\zeta}} \right) \\
&\leq -\frac{\lambda_i}{\delta_1 \cdots \delta_{i-1}} e_i^2 - s_{i-1} + s_i
\end{aligned}$$

which completes the proof of Lemma 4.2. ■

Proof of Lemma 4.3: Using (23), Definition 4.1 and Lemma A.1, the derivative of the quadratic function v_n in (24) can be written as

$$\begin{aligned}
\dot{v}_n &= e_n \frac{\theta_{n1}}{\delta_1 \cdots \delta_{n-1}} \dot{e}_n - \frac{1}{\delta_1 \cdots \delta_{n-1}} \sum_{\zeta=1}^j (\theta_{n\zeta} - \widehat{\theta}_{n\zeta}) \frac{\widehat{\theta}_{n\zeta}}{\rho_{n\zeta}} \\
&= e_n \frac{1}{\delta_1 \cdots \delta_{n-1}} \left[-\lambda_n e_n - \delta_{n-1} g_{n-1}(\mathbf{x}_{n-1}) e_{n-1} + \mathbf{Y}_n(\boldsymbol{\theta}_n - \widehat{\boldsymbol{\theta}}_n) \right] - \frac{1}{\delta_1 \cdots \delta_{n-1}} \sum_{\zeta=1}^j (\theta_{n\zeta} - \widehat{\theta}_{n\zeta}) \frac{\widehat{\theta}_{n\zeta}}{\rho_{n\zeta}} \\
&= -\frac{\lambda_n}{\delta_1 \cdots \delta_{n-1}} e_n^2 - \frac{1}{\delta_1 \cdots \delta_{n-2}} g_{n-1}(\mathbf{x}_{n-1}) e_{n-1} e_n + \frac{1}{\delta_1 \cdots \delta_{n-1}} \sum_{\zeta=1}^j (\theta_{n\zeta} - \widehat{\theta}_{n\zeta}) \left(p_{n\zeta} - \frac{\widehat{\theta}_{n\zeta}}{\rho_{n\zeta}} \right) \\
&\leq -\frac{\lambda_n}{\delta_1 \cdots \delta_{n-1}} e_n^2 - s_{n-1}
\end{aligned}$$

which completes the proof of Lemma 4.3. ■

REFERENCES

- [1] J.-J. E. Slotine and W. Li, *Applied nonlinear control*, Prentice-Hall Englewood Cliffs, NJ, 1991.
- [2] S. Skogestad and I. Postlethwaite, *Multivariable feedback control: analysis and design*, vol. 2, New York: Wiley, 2007.
- [3] W.-H. Zhu, *Virtual Decomposition Control - Toward Hyper Degrees of Freedom Robots*, Springer-Verlag, 2010.
- [4] L. Hunt, R. Su, and G. Meyer, "Global transformations of nonlinear systems," *IEEE Trans. Autom. Control*, vol. 28, no. 1, pp. 24–31, 1983.
- [5] M. Krstić, I. Kanellakopoulos, and P. Kokotović, *Nonlinear and Adaptive Control Design*, John Wiley & Sons, Inc., 1995.
- [6] D. Swaroop, J. K. Hedrick, P. P. Yip, and J. C. Gerdes, "Dynamic surface control for a class of nonlinear systems," *IEEE Trans. Autom. Control*, vol. 45, no. 10, pp. 1893–1899, 2000.
- [7] B. Song and J. K. Hedrick, *Dynamic surface control of uncertain nonlinear systems: an LMI approach*, Springer Science & Business Media, 2011.
- [8] P. P. Yip and J. K. Hedrick, "Adaptive dynamic surface control: a simplified algorithm for adaptive backstepping control of nonlinear systems," *Int. J. Control*, vol. 71, no. 5, pp. 959–979, 1998.
- [9] D. Wang and J. Huang, "Neural network-based adaptive dynamic surface control for a class of uncertain nonlinear systems in strict-feedback form," *IEEE Trans. Neural Netw.*, vol. 16, no. 1, pp. 195–202, 2005.
- [10] J.-J. Slotine and J. K. Hedrick, "Robust input-output feedback linearization," *Int. J. control*, vol. 57, no. 5, pp. 1133–1139, 1993.
- [11] M. Won and J. K. Hedrick, "Multiple-surface sliding control of a class of uncertain nonlinear systems," *Int. J. Control*, vol. 64, no. 4, pp. 693–706, 1996.
- [12] W.-H. Zhu, Y.-G. Xi, Z.-J. Zhang, Z. Bien, and J. De Schutter, "Virtual decomposition based control for generalized high dimensional robotic systems with complicated structure," *IEEE Trans. Robot. Autom.*, vol. 13, no. 3, pp. 411–436, 1997.
- [13] S. Mastellone and A. van Delft, "The impact of control research on industrial innovation: What would it take to make it happen?," *Control Engineering Practice*, vol. 111, pp. 104737, 2021.
- [14] J. Mattila, J. Koivumäki, D. Caldwell, and C. Semini, "A survey on control of hydraulic robotic manipulators with projection to future trends," *IEEE/ASME Trans. Mechatronics*, vol. 22, no. 2, pp. 669–680, 2017.

- [15] J. Koivumäki and J. Mattila, "Adaptive and nonlinear control of discharge pressure for variable displacement axial piston pumps," *J. Dyn. Sys., Meas., Control*, vol. 139, no. 10, pp. 101008, 2017.
- [16] P. Seiler and A. Alleyne, "Dissipative adaptive control for strict feedback form systems," *Eur. J. Control*, vol. 8, no. 5, pp. 435–444, 2002.
- [17] W.-H. Zhu and J. De Schutter, "Adaptive control of mixed rigid/flexible joint robot manipulators based on virtual decomposition," *IEEE Trans. Robot. Autom.*, vol. 15, no. 2, pp. 310–317, 1999.
- [18] H.K. Khalil, *Nonlinear systems*, Prentice Hall, 3rd edition, 2002.